






## ARTICLE

# Additive manufacturing of green composites: Poly (lactic acid) reinforced with keratin materials obtained from Angora rabbit hair

Cynthia Graciela Flores-Hernandez<sup>1</sup>  | Carlos Velasco-Santos<sup>1</sup>  |  
 José Luis Rivera-Armenta<sup>2</sup>  | Oscar Gomez-Guzman<sup>1</sup> |  
 José Martín Yañez-Limon<sup>3</sup> | Imelda Olivas-Armendariz<sup>4</sup> |  
 Juventino Lopez-Barroso<sup>1</sup>  | Ana Laura Martínez-Hernández<sup>1</sup> 

<sup>1</sup>División de Estudios de Posgrado e Investigación Av. Tecnológico s/n Esq. Gral. Mariano Escobedo, Tecnológico Nacional de México campus Querétaro, Querétaro, Mexico

<sup>2</sup>Tecnológico Nacional de México campus Ciudad Madero, Centro de Investigación en Petroquímica, Prolongación Bahía de Aldahir y avenida de las bahías, Altamira, Tamaulipas, Mexico

<sup>3</sup>Cinvestav Querétaro, Libramiento Norponiente 2000, Fraccionamiento Real de Juriquilla, Querétaro, Mexico

<sup>4</sup>Instituto de Ingeniería y Tecnología, Universidad Autónoma de Cd. Juárez, Chihuahua, Mexico

## Correspondence

Ana Laura Martínez-Hernández,  
 Tecnológico Nacional de México campus Querétaro, División de Estudios de Posgrado e Investigación Av. Tecnológico s/n Esq. Gral. Mariano Escobedo, Col. Centro Histórico, 76000, Querétaro, México.  
 Email: almh72@gmail.com

## Funding information

Tecnológico Nacional de México, Grant/Award Number: 6042.19-P

## Abstract

In this research, additive manufacturing of polylactic acid (PLA) reinforced with keratin was studied. Keratin was obtained from Angora rabbit hair and modified with NaOH. Scanning electron microscopy (SEM) images showed that the modified surfaces were rougher than untreated surfaces. Furthermore, SEM images in the composites' fracture regions showed surface changes, associated with the nature of the reinforcement. Likewise, thermomechanical properties of the composites were attributed to the nature of the reinforcement and the type of keratin. Besides, the 3D printed composites showed higher thermal conductivity values than PLA with the addition of keratin. Cytotoxicity tests revealed an improvement in cell growth compared to the control and PLA. These results are meaningful toward the development of high thermal conductors and biocompatible composites with applications in different fields, where the use of only natural polymers is necessary.

## KEYWORDS

biopolymers and renewable polymers, composites, microscopy, manufacturing, thermal properties

## 1 | INTRODUCTION

The field of 3D printing, also called additive manufacturing, has been growing exponentially in the last few years. As a result of its effortless operation, this technology promises to create sophisticated products at low costs,

improving the design and manufacturing, drastically shortening supply chains, and reducing waste production.<sup>1,2</sup> 3D printing (3DP) can be applied to various manufacturing markets and could potentially serve as a substitute for conventional processes. Furthermore, 3DP allows for the realization of complex freeform geometries,

as the process is not constrained by technological limitations of conventional manufacturing processes.<sup>3</sup>

3DP technology offers enormous potential in the biomedical industry, such as anatomical models for surgery training/planning, rehabilitation, dentistry, customized implants, drug delivery devices, and organ printing.<sup>4</sup> For example, additive manufacturing allows for the development of composites, which could be useful for biomaterials, such as those used for tissue engineering and possibly bone regeneration.<sup>5</sup> Green options for materials that can be used in 3D printing are emerging, such as polylactic acid (PLA).<sup>6</sup> PLA is a biodegradable, thermoplastic, aliphatic polyester which can be derived from renewable resources, such as starch, and is a sustainable alternative to petrochemically-derived products. Additionally, it exhibits high stiffness and strength and, consequently, is being used in several applications, such as food packaging, water and milk bottles, and degradable plastic bags, as well as in automotive applications.<sup>7</sup> However, PLA has a low tenacity, which is limiting in high mechanical demand applications, making improvement of these properties a desirable pursuit. The benefit of incorporating natural fibers into PLA for additive manufacturing has increased in recent years, mainly due to sustainability issues.<sup>8,9</sup> For example, natural waste materials can be used as reinforcements for composites, extending the life cycle of the waste, making the materials sustainable, biodegradable, and environmentally friendly.<sup>10,11</sup> PLA composites reinforced with natural fibers, such as wood, kenaf, and keratin, have displayed notable thermal and mechanical properties.<sup>9–13</sup> This has allowed the development of some materials that already exist on the market, such as biodegradable urns from PLA and flax, PLA-kenaf mobile phone cases, and in the automotive industry, the development and application of covers for replacement tires from PLA-kenaf fiber.<sup>14</sup> Therefore, investigating the use of other natural fibers as reinforcement alternatives to PLA, from natural and waste materials, is extremely attractive. For example, keratin is one of the most abundant biopolymers and is widely distributed in animal hairs.<sup>15</sup> Angora is a keratinous textile material, obtained from the pelts of the long-haired Angora rabbit, and Angora fiber can be used in several ways. Angora fiber has a low density of about 1.15–1.18 g/cm<sup>3</sup>, compared to 1.33 g/cm<sup>3</sup> for wool and 1.50 g/cm<sup>3</sup> for cotton. Further, the fiber's tenacity is around 14 cN/tex, and the breaking extension is 40%.<sup>16,17</sup> Angora fiber has a protein chemical structure that consists of spindle-shaped cortical cells. In fact, it is one of the world's warmest, softest, and lightest natural fibers, while still providing high insulation and a warmer feeling in garments, due to medulla structure in the core of the fiber.<sup>17</sup> On the other hand, the thermal conductivity

registered in rabbit hair is 35–37 mW/mK, suggesting an alternative use for rabbit fur as a sustainable and friendly material in the textile industry.<sup>18</sup>

Therefore, although there are different research studies on the use of natural fibers as reinforcements for composites and the use of keratin as a reinforcement material has already been studied, each keratin source offers different structures and, therefore, the possibility to diversify composite properties. Thus, keratin obtained from rabbit hair has not been studied as a reinforcement of PLA, especially using additive manufacturing to obtain biocomposites. This work is focused on the development, study, and analysis of a novel natural composite from PLA and Angora rabbit hair, processed by additive manufacturing. Further, we report thermal, thermo-mechanical, morphological, and cytotoxicity properties related to the amount of reinforcement used and the chemical nature of the reinforcements.

## 2 | EXPERIMENTAL

### 2.1 | Materials and methods

Angora rabbit hair was donated by Valentino's farm (Querétaro, México). PLA filament of natural color, with a 1.8 mm caliber, was used from trademark Print Filament. Sodium hydroxide (NaOH) was used to modify the surface of the ground rabbit hair and was purchased from Sigma-Aldrich.

### 2.2 | Sodium hydroxide treatment

One gram of ground rabbit hair was placed in a glass vessel, and 100 ml of 0.1 M NaOH was added to the vessel, followed by mechanical stirring. The mixture was heated to 50°C for 1 or 5 h (two different treatments). Then, the biofiber was separated from the solution and washed with distilled water to remove the excess NaOH (pH = 11), according to previous work done from our group.<sup>13</sup> Afterward, the rabbit hair was dried at 35°C for 48 h before preparing the blends for extrusion and additive manufacturing.

### 2.3 | Preparation of composites

The biocomposites were fabricated by extrusion and 3D printing. First, PLA-ground rabbit hair and PLA-treated ground rabbit hair (1 or 5 h at 50°C; 0.5, 1, or 2.5 weight percent [wt %]) were mixed in a glass vessel and fed into a Filabot extruder at a uniform temperature of 172°C.

Filaments for both kinds of composites ( $1.8 \pm 0.3$  mm diameter) were obtained in this way. Afterward, the shapes of the 3D test pieces were modeled using Solidworks software. CURA software was used to analyze STL-files. The composites were manufactured using a 3D printer (Industria 55, Queretaro, México) with a 1.5 mm diameter nozzle, a print speed of 850 mm/s, a nozzle temperature of 190°C, and room temperature in the print bed. The framework was 100% dense, with a 45° orientation, alternating between layers and layers, with respect to the axis of the piece.

Table 1 shows the corresponding concentration and nomenclature used in the manufacturing and characterization of composites, and Figure 1 shows the printed specimens. Test pieces of different shapes were prepared by 3D printing for analysis.

## 2.4 | Cell viability

Cell viability was evaluated using 3-(4,5-dimethylthiazol-2-yl)-2,5-diphenyltetrazolium bromide (MTT).<sup>19</sup> The samples were cultured and incubated with 10,000 mouse fibroblast cells (3 T3, ATCC®) in D-MEM with 10% fetal bovine serum (FBS) and 1% penicillin–streptomycin at 37°C. After 24 h, the culture medium was discarded, and 200 µL of D-MEM solution, supplemented with antibiotics, FBS, and 50 µL of MTT (5 mg/ml of phosphate buffer solution [PBS], 1X), were added. Then, the samples were incubated at 37°C for 3 h. After, the medium was discarded, and dimethyl sulfoxide (DMSO) was added to the dissolved formazan crystals. The absorbance of the solution was measured at 570 nm with a microplate reader. All measurements were completed using a microplate spectrophotometer (Benchmark Plus) and were carried out in triplicate. For cell morphology examinations, the cultured samples were stained with 4',6-diamidinophenyl-indol (DAPI; cell nuclei) and Calcein AM (cellular cytoplasm) solutions. Cell viability was expressed as a percentage relative to the control cells. Results are expressed as an average of three measurements, and the variability is reported as the standard deviation.

## 2.5 | Characterization

The morphology of composites was observed by scanning electron microscopy (SEM) using a TM-1000 de Hitachi microscope at an accelerating voltage of 15 kV. Rectangular 3D-printed samples ( $40 \times 1 \times 4$  mm) were fractured with N<sub>2</sub>, mounted on metal stubs and vacuum-coated with gold using a sputter coater (DENTON VACUUM Desk V HP). Simultaneous thermal analyses were carried out using a TA Instrument, model Q600; samples were heated at 10 °C/min under a N<sub>2</sub> gas atmosphere from room temperature up to 600°C with a N<sub>2</sub> flow rate of 100 ml/min. The rectangular PLA-reinforced 3D-printed samples were analyzed by dynamical mechanical analysis (DMA; TA instruments Q800) using dual cantilever mode with a frequency of 1 Hz over 30–200°C, with a heating rate of 5°C/min. Thermal diffusivity, specific heat (Cp),

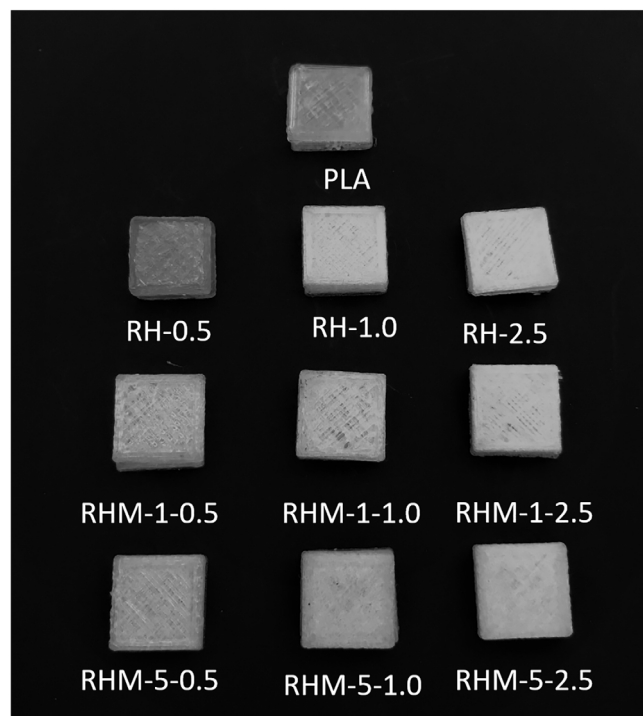


**FIGURE 1** Image of printed specimens for composites with 0–5 wt% of rabbit hair and PLA. PLA, polylactic acid [Color figure can be viewed at [wileyonlinelibrary.com](http://wileyonlinelibrary.com)]

**TABLE 1** Composition and nomenclature of PLA/keratin reinforced composites

Percentage of Angora rabbit hair (RH) reinforcement (wt %)	Type of Keratin reinforcement		
	Without treatment	Treated 1 (50 °C – 1 h)	Treated 2 (50 °C – 5 h)
0.5%	RH-0.5	RHM-1-0.5	RHM-5-0.5
1%	RH-1.0	RHM-1-1.0	RHM-5-1.0
2.5%	RH-2.5	RHM-1-2.5	RHM-5-2.5

and thermal conductivity (thermal analysis) were measured with laser flash equipment (Linseis LFA-1000). All analyses were made at room temperature under vacuum ( $10^{-3}$  mtorr) with a Nd:YAG laser ( $25 \text{ mJ pulse}^{-1}$ ) and variable pulse length. Quadrangular 3D-printed samples were manufactured in sizes of  $10 \times 2 \times 10 \text{ mm}$ . The design of experiment (DOE) was performed to evaluate data thermal conductivity using Minitab 17. This experiment is designed considering two factors: treatment (3 level) and concentration (4 level; see supplementary information).

### 3 | RESULTS AND DISCUSSION

#### 3.1 | Morphology of fibers and composites

The difference between rabbit hair fiber with and without chemical treatment at different times is shown in Figure 2. Images a) and b) show rabbit hair without

treatment. The longitudinal surface of the fiber clearly presents the characteristic of rabbit fibers, with chevrons pointing out to the principal axis of the fiber, as previously noted.<sup>15,20</sup> The ends of the fibers remain closed, preventing any material from entering them. After, NaOH chemical treatment for 1 h, the fibers undergo slight erosion over their entire surface (Figures 2(c),(d)). However, they still maintain the primary characteristic of rabbit hair fiber, the length and diameter ratio. The fibers treated for 5 h (Figures 2(e-f)) show a surface with more apparent damage along the fiber, exhibiting roughness in the fiber edge surrounded by groove patterns and completely open tips. Hence, treatment time seems to directly influence surface roughness. Therefore, this is considered a more aggressive procedure compared to helium (He) or  $\text{He}^+$  air plasma treatment<sup>17</sup> but remarkably like ozone treatment, in which the outer layer of the fiber is also damaged.<sup>16</sup> Finally, NaOH treatment exhibits more invasive behavior toward the keratin material present in rabbit hair (predominantly  $\alpha$ )<sup>21</sup> than that reported in chicken feathers (predominantly  $\beta$ )<sup>22,23</sup> under the

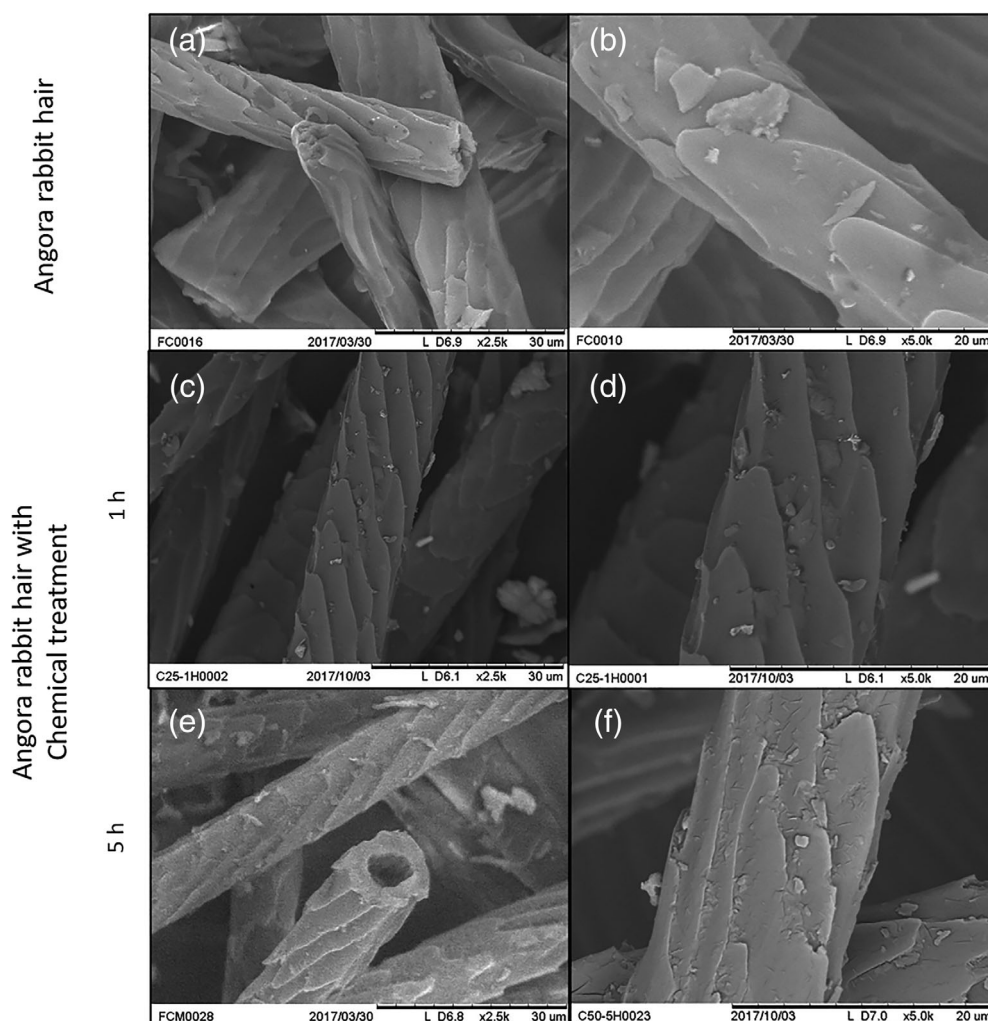


**FIGURE 2** Scanning electron microscopy (SEM) micrographs. Surface appearance of Angora rabbit hair (RH): (a, b) without treatment; (c, d) with chemical treatment of NaOH by 1 h (RHM-1) and (e, f) with chemical treatment of NaOH by 5 h (RHM-5)

same time and mercerization conditions. However, chemical treatment meets the objective, changing the surface topography needed to improve the link in the composites at the interface level with PLA,<sup>22,24–27</sup> unlike plasma treatments used in other investigations,<sup>28</sup> where no defects or tears were observed when comparing images obtained before and after treatment. Thus, current research is evaluating other properties, not considered in this article, investigating the implications of both treatments (NaOH at 1 and 5 h) and the repercussions of roughness produced by chemical treatment on the surface for other composite properties.

Figure 3 shows SEM micrographs of the fracture surface with N<sub>2</sub> of the PLA, PLA-angora fiber (RH-2.5), and PLA-treated angora fiber (RHM-1-2.5, RHM-5-2.5). In Figures 3(a),(b), the fracture surface obtained from PLA can be observed. Cavities that appear in the first images are attributed to the 3D printing movement, which is related to the nozzle diameter and speed of printing; these factors influence the final application of the printed material.<sup>29</sup> A smooth surface is also observed between the layers of the PLA material.<sup>7</sup>

Figures 3(c–e) show the fracture surfaces of reinforced composites, allowing the way the reinforcements influence the composites to be observed. In fractures of composites reinforced with treated fibers, the affected areas present different relief compared with polymers from unmodified fibers. Composites also show differences in the print direction patterns. Fractures of untreated fiber-reinforced composites have a homogeneous surface, attributed to good

adhesion between the reinforcement and matrix. This behavior could be related to results previously obtained in DMA, corresponding to the registration of the largest storage modules in composites reinforced with untreated rabbit hair. On the other hand, the fracture of the fiber-reinforced composite treated for 1 h shows a rupture pattern that is not present in PLA or fiber-reinforced composites without treatment. The river patterns present in the fracture surface suggest a toughening effect in PLA, coinciding with the decrease in the storage module for the reinforced composites after 1 h of treatment.<sup>30,31</sup> The image of the fracture of the fiber-reinforced composite treated for 5 h (2.5 wt %; Figure 3e) shows holes generated by 3D printing, in addition to fiber agglomerations, which could correspond to irregular dispersion, reflected in thermal conductivity (discussed in a later section) because a clear decrease in K is shown in these composites compared with composites reinforced with untreated fibers and fibers treated for 1 h. Finally, images of the fractures suggest that the nature of the reinforcement is an important parameter in the obtained results; the images of the fracture surface of the fiber-reinforced composites without chemical treatment show good dispersion and fiber wettability by the polymer, without agglomerations or saturations.

### 3.2 | Thermal analysis

Material thermal analysis identifies thermal stability of the prepared composites, in addition to evaluating

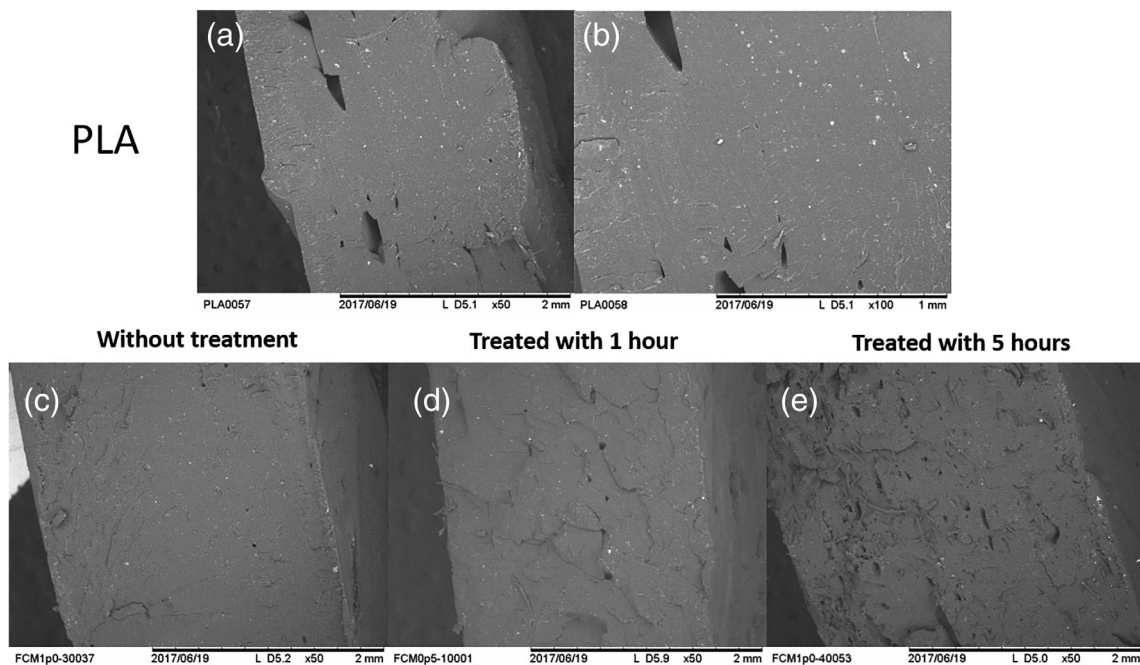


**FIGURE 3** SEM images of angora rabbit hair-PLA composites. SEM, scanning electron microscopy

thermal degradation of the composites and its critical role in the final composite performance. Figure 4a shows the weight loss and heat flow curves for PLA-keratin rabbit hair composites. The three graphs obtained by thermal analysis (differential scanning calorimetry; DSC) are

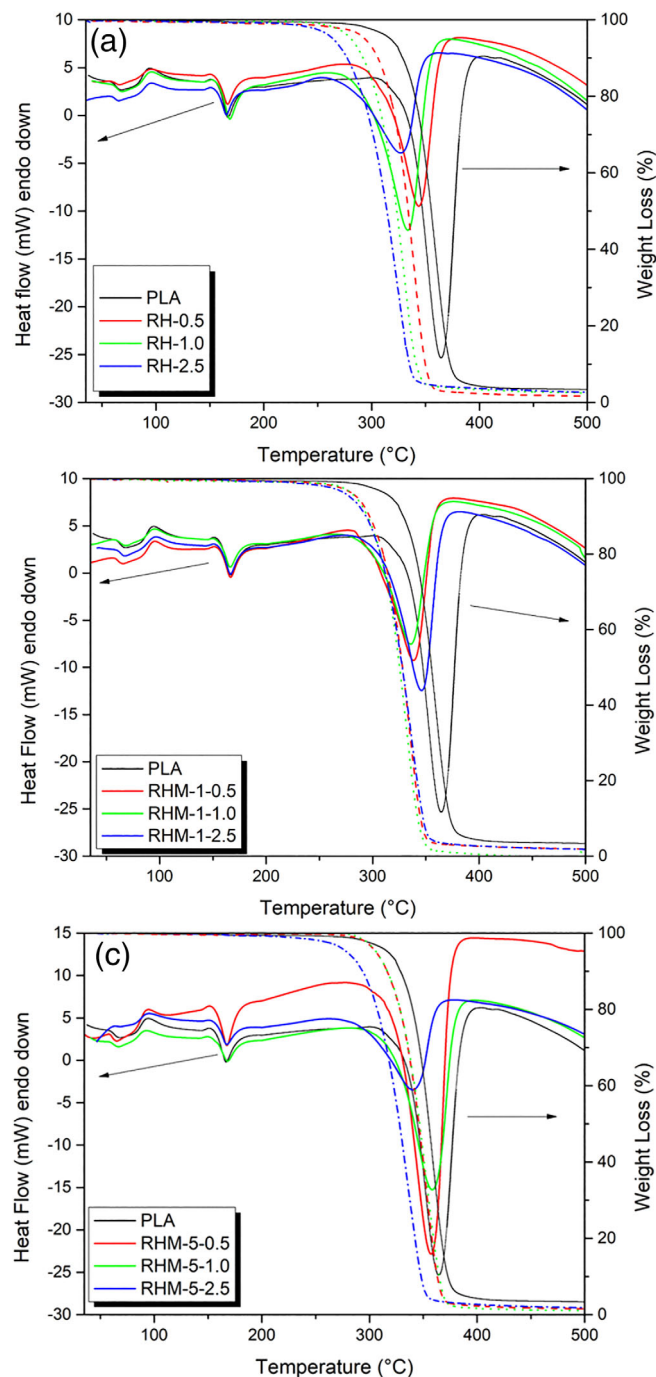


**FIGURE 4** DSC-TGA curves for composites with: (a) composites reinforced with rabbit hair; (b) composites reinforced with rabbit hair modified by 1 h; (c) composites reinforced with rabbit hair modified by 5 h. DSC, differential scanning calorimetry; TGA, thermogravimetric analysis [Color figure can be viewed at [wileyonlinelibrary.com](http://wileyonlinelibrary.com)]

similar. The glass transition temperature was found around 60°C, and cold crystallization occurred between 85 and 101°C.<sup>32,33</sup> The endothermic peak around at 170°C could be associated with the melting temperature of PLA, which has been reported in this range.<sup>29,32–34</sup> On the other hand, the temperature range obtained for melting of the reinforced composites is below the denaturation temperature range for alpha-keratin (230–248°C),<sup>35,36</sup> which has also been reported to change with humidity (155–205°C).<sup>37</sup> Considering the thermal processing conditions for the PLA-Angora rabbit hair composites, humidity present in the reinforcement should be low. Therefore, the structure of keratin still prevails and, therefore, also influences the decomposition temperature. The next endothermic peak in the DSC for the PLA and composites at 345–365°C can be attributed to total decomposition of the composites. This temperature range agrees with the highest weight loss observed during thermogravimetric analysis (TGA; discussed in the following paragraphs). Moreover, when the amount of rabbit hair increases, the decomposition peak decreases in intensity, indicating that decomposition of the material is easier to carry out; the  $\Delta H_d$  (decomposition enthalpy, reported in Table 2) corroborated this fact. Additionally, the melting enthalpy ( $\Delta H_m$ ) for PLA is approximately 56 J g<sup>-1</sup>, and the reinforced composites show a  $\Delta H_m$  decrease up to 36 J g<sup>-1</sup> with the addition of keratin (sample RH-2.5 in Figure 4a). Similar behavior has been reported in other investigations.<sup>38</sup>

The most significant change is observed in the last endothermic peak of each graph (see Figures 4(a–c)), where a decrease in decomposition temperature, depending on chemical nature of the reinforcement, is shown. This peak is smaller for composites reinforced with keratin and chemically modified for longer times (5 h) and with the highest keratin concentrations (RHM-5-2.5). For this polymer composite, a peak (340°C), 25°C lower than that for PLA (365°C), is obtained, as well. This behavior may be related to the SEM images described before, arising due to the chemical reaction, which damages the keratin surface and influences its thermal response at lower temperatures than the matrix.

The thermal behavior of PLA and keratin composites obtained by additive manufacturing was also examined by TGA. Figures 4(a–c) show TGA curves for composites reinforced with keratin, both without modification and modified at 1 and 5 h, comparing their behavior to pristine PLA.

The three curves have nearly identical behaviors. The foremost degradation step occurs from 270–380°C, ascribed to composite thermal degradation. The weight loss percentage is mainly attributed to depolymerization of the PLA ester bonds.<sup>34,39–43</sup> Finally, a residue of

**TABLE 2** Melting ( $T_m$ ) and Decomposition ( $T_d$ ) temperature and related enthalpies obtained from DSC curves in thermal analysis

Materials	$T_m / ^\circ\text{C}$	$\Delta H_m = (\text{J g}^{-1})$	$T_d / ^\circ\text{C}$	$\Delta H_d = (\text{J g}^{-1})$
PLA	167	56	365	904
RH-0.5	166	43	345	488
RH-1.0	169	56	334	636
RH-2.5	165	36	327	187
RHM-1-0.5	167	42	338	441
RHM-1-1.0	166	43	336	356
RHM-1-2.5	167	43	346	546
RHM-5-0.5	167	56	357	1147
RHM-5-1.0	168	43	358	704
RHM-5-2.5	167	42	340	294

approximately 2–4% by weight was observed at 600°C. On the other hand, a slight decrease in the degradation temperature was observed in most cases, as the reinforcement content increased in the composites. Thus, the PLA crystalline zones seem to be influenced by keratin fibers, in general (treated and untreated); this effect is corroborated in the decreased melting enthalpy ( $\Delta H_m$ ; Table 2). In addition, amorphous areas were also influenced by the presence of keratin, as observed by the decrease in decomposition composition enthalpies. Therefore, the decrease in crystalline domains present in the polymer composites of PLA-keratin generate the decrease in the matrix's thermal stability. In addition, there are investigations of natural fiber-reinforced PLA composites, reporting decreases in thermal stability. These reports indicate that natural fibers swell in alkaline medium, which causes a decrease in thermal resistance, but the crystalline phase is not modified. However, this behavior allows the amorphous regions to degrade more easily.<sup>43–45</sup> As mentioned, in this investigation, crystallinity seems to be affected. Finally, the TGA results are related to the endothermic DSC peaks, as described above, and the effect on the thermal resistance of polymer composites is verified. Therefore, in most of the materials, the chemical treatment carried out on keratin affects its relationship with the decreased thermal stability after modification with NaOH.

### 3.3 | Thermo-mechanical analysis

Storage modulus ( $E'$ ) and tan delta ( $\tan \delta$ ), as a function of the PLA temperatures and the composites, are shown in Figures 5(a–f). The graph in (a) shows the results of  $E'$  obtained from the reinforced composites with unmodified rabbit hair; and the highest  $E'$  value for these composites (200 GPa at 35°C) is obtained in sample RH-2.5, which is lower than PLA ( $E' = 280$  GPa at 35°C).

This behavior can be ascribed to  $\alpha$ -keratin in rabbit hair, which is flexible and promotes lower rigidity in these composites.<sup>46,47</sup> Other polymer composites developed from materials with predominantly  $\beta$ -keratin,<sup>21</sup> obtained from chicken feathers, have a tendency to be more rigid compared to the natural polymer matrix processed by methods other than 3D printing.<sup>22,23,48</sup>

Figures 5(b),(c) also show lower  $E'$  values for composites reinforced with modified keratin compared to PLA. Besides, in most of these samples,  $E'$  is lower than values obtained for composites with unmodified keratin. Therefore, the results suggest that chemical treatments improve interactions between the polymer matrix and keratin, giving the composites more flexibility, which is a characteristic property of  $\alpha$ -keratin.

Figures 5(d–f) show  $\tan \delta$  curves for composites and PLA. This damping parameter ( $\tan \delta$ ) is the ratio of loss and storage moduli.<sup>48</sup> In Figure 5(d), the glass transition temperature ( $T_g$ ) of PLA is observed around 67°C, and the  $T_g$  values of composites with unmodified hair are around 64, 70, and 66°C for composites with 0.5, 1.0, and 2.5 wt %, respectively. Therefore, the increase in  $T_g$  in reinforced composites is minimal and only occurs with 1 wt % reinforcement material. On the other hand,  $\tan \delta$  values are lower than PLA (1.05) in reinforced composites (see Table 3). Lower  $\tan \delta$  values in all composites compared to PLA are related to the resistance to movement of polymeric chains linked to keratin. Consequently, friction between the chains is diminished in the presence of reinforcement, as reported in other investigations.<sup>8,39,49,50</sup> Thus, having smaller energy dissipation coefficients in the composites indicates a strong interaction between the fiber and matrix, allowing characteristics presented by keratin reinforcement, such as flexibility, to be transmitted to PLA.<sup>50</sup>

In Figures 5(e),(f), the same behavior as observed in Figure 5(d) can be appreciated; the composites have lower storage potential for energy than heat dissipation

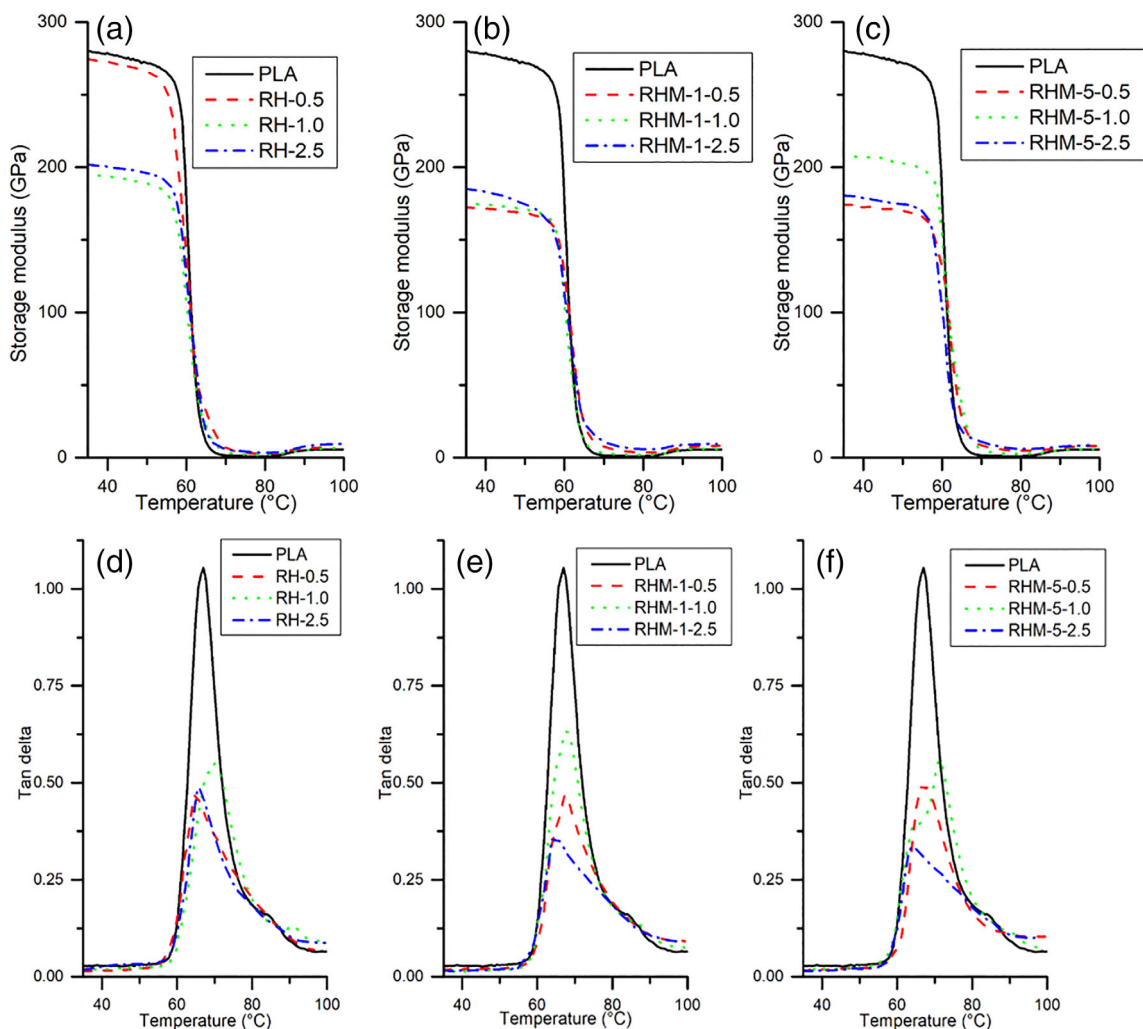


**FIGURE 5** Storage modulus ( $E'$ ) for composites with: (a) composite reinforced with rabbit hair; (b) composite reinforced with rabbit hair modified by 1 h; (c) composite reinforced with rabbit hair modified by 5 h. Tan  $\delta$  curves for composites with: (d) composite reinforced with rabbit hair; (e) composite reinforced with rabbit hair modified by 1 h; (f) composite reinforced with rabbit hair modified by 5 h [Color figure can be viewed at [wileyonlinelibrary.com](http://wileyonlinelibrary.com)]

**TABLE 3** Tan  $\delta$  and  $T_g$  of composites with 0.5–2.5% of Angora rabbit hair and treated Angora rabbit hair

Sample	Tan $\delta$	$T_g$ , °C
PLA	1.05	67
RH-0.5	0.46	65
RH-1.0	0.54	70
RH-2.5	0.49	66
RHM-0.5	0.47	67
RHM-1.0	0.63	68
RHM-2.5	0.36	65
RHM-0.5	0.49	67
RHM-1.0	0.56	71
RHM-2.5	0.33	64

energy.<sup>40,50</sup> These results verified that the presence of keratin fiber in all the composites produces a reduction in the movement of polymeric chains and a decrease in the value of tan  $\delta$ . Furthermore, both suggest a better interface between the reinforcement and matrix.

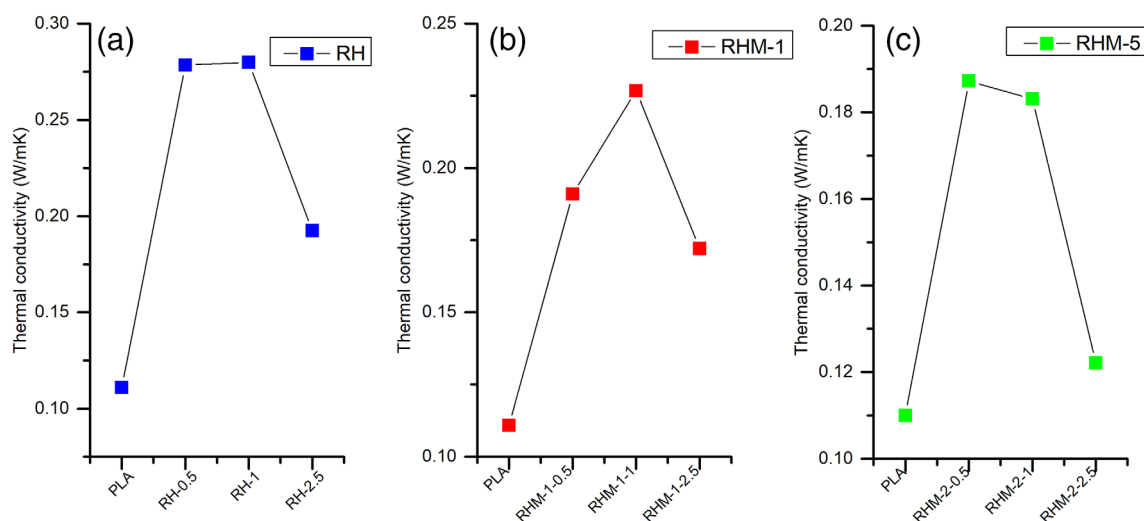
### 3.4 | Thermal conductivity

Thermal conductivity is a physical property of materials that measures the heat conduction ability or ability of a substance to transfer kinetic energy to substances with which it is in contact. A material with low thermal conductivity is considered insulating. In contrast, if the material has high conductivity, it is considered a heat conductor.<sup>51</sup> In Table 4, the properties of thermal



**TABLE 4** Thermal properties of composites with 0.5–2.5% of Angora rabbit hair and treated Angora

	(m <sup>2</sup> /s) Diffusivity	(J/gK) Cp	(g/m <sup>3</sup> ) ρ × 10 <sup>6</sup>	(W/mK) K
PLA	1.02E-07	0.91	1.19	0.111
RH-0.5	2.31E-07	1.22	0.99	0.278
RH-1.0	2.10E-07	1.28	1.04	0.280
RH-2.5	2.60E-07	0.96	0.76	0.192
RHM-1-0.5	1.81E-07	1.27	0.829	0.191
RHM-1-1.0	2.50E-07	1.42	0.63	0.227
RHM-1-2.5	1.76E-07	0.94	1.044	0.172
RHM-5-0.5	2.02E-07	1.18	0.78	0.187
RHM-5-1.0	1.71E-07	1.03	1.04	0.183
RHM-5-2.5	1.32E-07	1.14	0.81	0.122

**FIGURE 6** Thermal conductivity for composites: (a) composite reinforced with rabbit hair; (b) composite reinforced with rabbit hair modified by 1 h; (c) composite reinforced with rabbit hair modified by 5 h ( $S = 0.014$  see supplementary) [Color figure can be viewed at [wileyonlinelibrary.com](http://wileyonlinelibrary.com)]

diffusivity ( $\alpha$ ),  $C_p$ , density, and thermal conductivity ( $K$ ) of the reinforced composites are observed. The parameter  $K$  is a transport property and is characteristic of the given material; it also provides an indication of the rate at which energy is transferred by the diffusion process.  $K$  is the product of thermal diffusivity ( $\alpha$ ), density ( $\rho$ ), and specific heat ( $C_p$ ).<sup>52</sup>

Figure 6 shows the thermal conductivity values ( $K$ ) obtained for PLA and composites processed by additive manufacturing. The three graphs involve the all the composites reinforced with rabbit hair, with and without modification. In Figure 6(a), ( $K$ ) values of 0.278, 0.280, and 0.192 W/mK are observed for composites with 0.5, 1.0, and 2.5 wt % of unmodified rabbit hair, respectively. All these  $K$  values are higher than that of the PLA matrix (0.111 W/mK). Therefore, keratin produces thermal conductive behavior in PLA and, as a result, is a better heat

conductor. However,  $K$  diminishes with the highest percentage of reinforcement (2.5 wt %); this behavior could be attributed to reinforcement, which seems to oversaturate the matrix, and the inadequate distribution of keratin, which modifies the thermal conductivity in the composites.

Regarding the specific heat, in the composite with the highest reinforcement concentration, which was modified for 5 h (RHM-5-2.5), we observe high values of  $C_p$ , which correspond to a low value of  $K$ . This can be attributed to the composite absorbing more energy than it transfers. On the other hand, thermal diffusivity in composites with high percentages of reinforcement (2.5 wt%) typically have the following behavior. In the composite with fiber, treated for 1 h (RHM-1-2.5), a slight decrease is observed, but the composite reinforced with fiber, treated for 5 h (RHM-5-2.5), shows a greater decrease in

thermal diffusivity. This can be attributed to the fact that concentration influences dispersion, and the chemical treatment carried out on the reinforcement generates wear on the fiber surface, which changes the surface, affecting thermal diffusivity and generating low values ( $RHM-5-2.5 = 1.32E-07 \text{ m}^2/\text{s}$ ). The reinforced composite with unmodified fiber (RH-2.5) has a smaller decrease than the fiber-treated composites, which is attributed to poor reinforcement dispersion in this case, where it is only influenced by concentration.

Composites included in Figure 6(b), reinforced with keratin modified with NaOH for 1 h, show thermal conductivity values of 0.191, 0.227, and 0.172 W/mK, depending on concentration. The behavior is similar to that shown in Figure 6(a). However, the conductivities are lower for each concentration of composite reinforced with unmodified keratin. However, in Figure 6(c) (composites reinforced with chemically-treated rabbit hair for 5 h), the maximum value of K is obtained with the lowest percentage of reinforcement (RHM-5-0.5,  $K = 0.187 \text{ W/mK}$ ) and composites with 1.0 and 2.5 wt % exhibited values of 0.183 and 0.122 W/mK, respectively. This behavior could be attributed to the chemical modification time for the rabbit hair, which modifies the surface and thermal properties significantly, as mentioned previously and analyzed with the described techniques (SEM, DSC, and DMA).

Finally, the presence of keratin contributes to the modification of PLA thermal conductivity, as well as chemical treatment, producing a diminished in K. These results are tangible (Figure 6), since compared to K values at the same concentration (for instance RH-0.5, RHM-1-0.5, and RHM-2-0.5) a decrease in K is observed for composites with the treatment conditions in rabbit hair. Thermal conductivity in keratin is associated with a well-organized structure and self-assembled protein.<sup>52</sup> The influence of factors, such as modification and concentration in the experiment, were validated using a factorial design. Figure S1 shows the interaction plot of the two factors. Based on this plot, we validated the significance of thermal conductivity values with interaction of reinforcement without chemical treatment and the lowest concentration of reinforcement ( $S = 0.014$ ). S represents the distance between the data and fitted values. The low value of S indicates that the result will better suit the model. According to the *P* value obtained in the ANOVA (less than 0.05; see Table S1 in supplementary information), the interaction of concentration and modification are significant, and there is no influence from error. Furthermore, the R-squared value for this analysis is 93.74%, confirming effective thermal conductivity measurements, indicating that the deviation of measured values is slight. The increase of thermal conductivity produced by keratin

in PLA composites could be a viable alternative to several techniques previously used to increase thermal conductivity in polymers through structure manipulation, self-assembly, alienation, and orientation of polymer chains.<sup>52</sup>

According to some investigations, the thermal conductivity value of PLA ranges, approximately, from 0.064–0.23 W/mK.<sup>53–56</sup> In this study, we report a value of 0.111 W / mK, within the reported range. On the other hand, other works have reported thermal conductivity value changes in keratin depending on its source (0.1924 W/mK for wool fibers,<sup>57</sup> 2.99 W/mC for wool, 2.49 W/m° C for goose down,<sup>58</sup> and  $3.8 \times 10^3 \text{ W/mK}$  for rabbit skin [with long hairs and dyed]).<sup>18</sup> Therefore, some kinds of keratin present higher values of thermal conductivity than PLA. Finally, the incorporation of keratin significantly influenced the thermal conductivity increase of the composites (0.122–0.28 W/mK).

### 3.5 | Cell viability

The functioning of a cell is affected mainly by its physical environment because cells must first adhere to a material before proliferating. Therefore, the biocompatible materials used (in this research, PLA and composites) should also have relevant properties, such as hydrophilic surfaces, wettability, and non-toxic effects.<sup>59</sup> PLA and keratin, alone or in combination with other biomaterials, have shown generally good compatibility with cells and tissues.<sup>60–64</sup> Figure 7 shows the proliferation, adhesion, and viability of fibroblasts cells on materials after 24 h cultures. Fluorescent microscopy of the material surfaces revealed a large number of adhered cells, with some being round in shape. In contrast, other cells partly spread, and some even aggregated, behavior which is related to the pores of the biomaterial surfaces.<sup>65</sup> Besides, the nuclei of fibroblasts (blue), enveloped by the cytoplasm, can be seen; similar results have been obtained in other investigations using 4',6-diamidinophenyl-indol (DAPI) as a fluorescent dye for the identification of fibroblast nuclei.<sup>66</sup>

On the other hand, the cells' cytoplasm, as well as cell–cell interactions, are clearly observable (using Calcein M), being appreciated around the cell nucleus, as indicated by a lower intensity blue color. Results agreed with the cell viability analysis, showing no sign of cytotoxicity in any of the materials. Furthermore, results were similar for human bone marrow mesenchymal stem cells cultured in biocomposites. These results were based on the combination of PLA polymer matrix with keratin additives, where the keratin concentration does not affect cell viability or the cell-material interaction.<sup>66</sup>

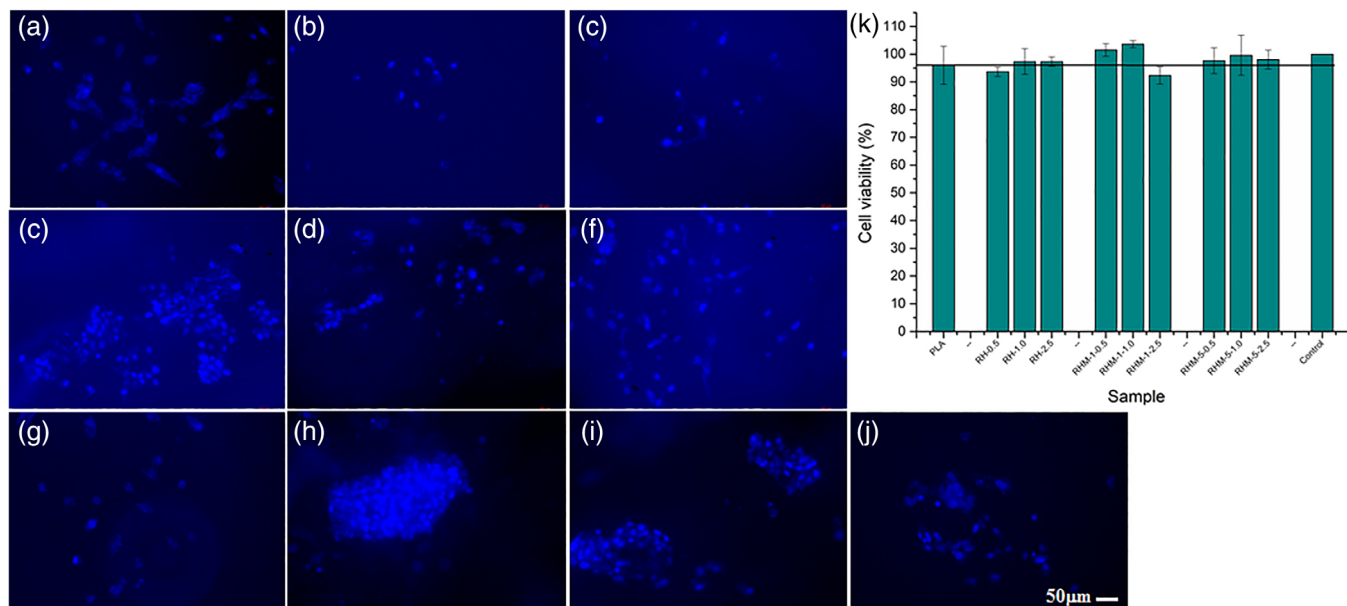


**FIGURE 7** Fluorescent microscopy images of adhesion and proliferation of fibroblast cells on materials and cell viability after 24 h of culturing. (a) RH-0.5, (b) RH-1.0, (c) RH-2.5, (d) RHM-1-0.5, (e) RHM-1-1.0, (f) RHM-1-2.5, (g) RHM-5-0.5, (h) RHM-5-1.0, (i) RHM-5-2.5, (j) Control, and (k) cell viability (%) of materials in 3 T3 fibroblasts cells by MTT assay [Color figure can be viewed at [wileyonlinelibrary.com](http://wileyonlinelibrary.com)]

## 4 | CONCLUSIONS

Composites reinforced with keratin and modified keratin from rabbit hair were obtained by additive manufacturing. According to the SEM results, chemical modification of the reinforcement with NaOH for 5 h causes some damage to the fiber surface. Compared with 1 h of chemical treatment, which produces moderate damage in the rabbit hair structure, this effect has moderate repercussions to the thermal conductivity. However, it is needed to verify if 5 h of treatment influences other properties, such as mechanical properties, where more surface roughness could be useful at the interface level. Thermal results obtained from DSC-TGA evidence changes with decomposition temperature for most of the composites (327–340°C), which is related to the increase in reinforcement and chemical treatment performed on the fiber. In addition, thermal conductivity of the composites increases up to 155% in the composites with unmodified rabbit hair. The energy dissipation coefficients in the composites indicate a link between the fiber and matrix.

Cytotoxicity tests show favorable cell growth in PLA, which is further improved by keratin incorporation (increasing up to 4%), indicating that keratin could diversify possible uses of PLA. On the other hand, additive manufacturing allows shapes to be built in three dimensions, influenced by keratin, which favors cell growth.

Also, it could be useful for the development of biomaterials for applications, such as tissue engineering. This is the first study that incorporates rabbit hair as a reinforcement for PLA using additive manufacturing. Finally, this work reinforces the direction of research focused on applications using waste materials as alternatives for eco-composite development.

## ACKNOWLEDGMENTS

The authors are grateful to Valentino's farm (Querétaro, México) and her owner Rene Christy for rabbit hair donation. To Mr. Rivelino Flores Fariás for his assistance in the analysis of thermal properties, and Dr. Marina Vega for her technical assistance in SEM. Authors are thankful for the financial support through the project TECNM 6042.19-P. In memoriam Dr Marisela Estefania Angeles-San Martin and Prof. Rosendo H. Martínez-Bautista.


## ORCID

Cynthia Graciela Flores-Hernandez <https://orcid.org/0000-0002-7863-8720>

Carlos Velasco-Santos <https://orcid.org/0000-0003-2743-8611>

José Luis Rivera-Armenta <https://orcid.org/0000-0002-9076-2353>

Juventino Lopez-Barroso <https://orcid.org/0000-0001-7954-135X>

Ana Laura Martinez-Hernandez  <https://orcid.org/0000-0001-7038-5303>

## REFERENCES

- [1] B. Kaynak, M. Spoerk, A. Shirole, W. Ziegler, J. Sapkota, *Macromol. Mater. Eng.* **2018**, 303(5), 1800037. <https://doi.org/10.1002/mame.201800037>.
- [2] B. Wendel, D. Rietzel, F. Kuhnlein, R. Feulner, G. Hulder, E. Schmachtenberg, *Macromol. Mater. Eng.* **2008**, 293, 799. <https://doi.org/10.1002/mame.200800121>.
- [3] M. Gebler, A. J. M. S. Uiterkamp, C. Visser, *Energy policy* **2014**, 74, 158. <https://doi.org/10.1016/j.enpol.2014.08.033>.
- [4] M. Touri, F. Kabirian, M. Saadati, S. Ramakrishna, M. Mozafari, *Adv.Eng. Mater.* **2019**, 1800511, 21. <https://doi.org/10.1002/adem.201800511>.
- [5] L. E. Rojas-Martínez, C. G. Flores-Hernandez, L. M. López-Marín, A. L. Martínez-Hernandez, S. B. Thorat, C. D. Reyes-Vasquez, A. E. Rio-Castillo, C. Velasco-Santos, *Eur. Polym. J.* **2020**, 141, 110088. <https://doi.org/10.1016/j.eurpolymj.2020.110088>.
- [6] I. Anderson, *3D Print. Addit. Manuf.* **2017**, 4(2), 110. <https://doi.org/10.1089/3dp.2016.0054>.
- [7] M. Joonobi, J. Harun, A. P. Mathew, K. Oksman, *Compos. Sci. Technol.* **2010**, 70(12), 1742. <https://doi.org/10.1016/j.compscitech.2010.07.005>.
- [8] R. Scaffaro, M. Morreale, F. Mirabella, F. P. La Mantia, *Macromol. Mater. Eng.* **2010**, 296, 141. <https://doi.org/10.1002/mame.201000221>.
- [9] J. A. Travieso-Rodríguez, M. D. Zandi, R. Jerez-Mesa, J. Lluma-Fuentes, *Mater. Res. Technol.* **2020**, 9(4), 8507. <https://doi.org/10.1016/j.jmrt.2020.06.003>.
- [10] A. M. Pringle, M. Rudnicki, J. M. Pearce, *For. Prod. J.* **2018**, 68(1), 86. <https://doi.org/10.13073/FPJ-D-17-00042>.
- [11] D. X. Zhao, X. Cai, G. Z. Shou, Y. Q. Gu, P. X. Wang, *Key Eng. Mater.* **2015**, 667, 250. <https://doi.org/10.3390/jcs4040159>.
- [12] S. Ochi, *Mech. Mater.* **2008**, 40, 446. <https://doi.org/10.1016/j.mechmat.2007.10.006>.
- [13] C. G. Flores-Hernandez, C. Velasco-Santos, A. L. Hernandez-Zea, O. Gomez-Guzman, J. M. Yañez-Limon, J. L. Rivera-Armenta, A. L. Martínez-Hernandez, *J. Nat. Fibers.* **2020**, 1. <https://doi.org/10.1080/15440478.2020.1788483>.
- [14] N. Graupner, A. S. Herrmann, J. Mussig, *Composites: Part A* **2009**, 40, 810. <https://doi.org/10.1016/j.compositesa.2009.04.003>.
- [15] D. Wang, X.-H. Yang, R.-C. Tang, F. Yao, *Polymer* **2018**, 10(993), 1. <https://doi.org/10.3390/polym10090993>.
- [16] S. Perincek, M. I. Bahtiyari, A. E. Korlu, K. Duran, *J. Cleaner Prod.* **2008**, 16, 1900. <https://doi.org/10.1016/j.jclepro.2008.01.005>.
- [17] N. Danish, M. K. Garg, R. S. Rane, P. B. Jhala, S. K. Nema, *Appl. Surf. Sci.* **2007**, 253, 6915. <https://doi.org/10.1016/j.apsusc.2007.02.015>.
- [18] L. Hes, in *In Book Biologically Inspire Textiles* (Eds: A. Abbott, M. Ellison), Woodhead Publishing Ltd, Abington **2008**, p. 150. <https://doi.org/10.1533/9781845695088.2.150>.
- [19] E. Diaz-Acosta, C. Rodriguez-Gonzalez, L. Valencia-Gomez, S. A. Martel-Estrada, M. Hernandez-Gonzalez, H. Reyes-Blas, *I. J. Appl. Pack. Res.* **2018**, 10(3), 70.
- [20] W. Broeck, P. Moertier, P. Simoens, *Folia Morphol.* **2001**, 60-1, 33.
- [21] B. Wang, W. Yang, J. McKittrick, M. A. Meyers, *Prog. Mater. Sci.* **2016**, 76, 229. <https://doi.org/10.1016/j.pmatsci.2015.06.001>.
- [22] C. G. Flores-Hernandez, A. Colin-Cruz, C. Velasco-Santos, V. M. Castaño, A. Almendarez-Camarillo, I. Olivas-Armendariz, A. L. Martínez-Hernandez, *Polym. Environ.* **2018a**, 26-5, 2182. <https://doi.org/10.1007/s10924-017-1115-1>.
- [23] C. G. Flores-Hernandez, A. L. Martínez-Hernandez, A. Colin-Cruz, F. Martínez-Bustos, V. M. Castaño, I. Olivas-Armendariz, A. Almendarez-Camarillo, *Starch/Starke* **2018b**, 11-12(1700295), 70. <https://doi.org/10.1002/star.201700295>.
- [24] A. O'Donnell, M. A. Dweib, R. P. Wool, *Compos. Sci. Technol.* **2004**, 64, 1135. <https://doi.org/10.1016/j.compscitech.2003.09.02>.
- [25] M. Das, D. Chakraborty, *J. Appl. Polym. Sci.* **2006**, 102, 5050. <https://doi.org/10.1002/app.25105>.
- [26] Van de Weyenberg, I.; Truong, T.C.; Vangrimde, B.; Verpoest, I. *Compos. A.* **2006**, 37, 1368–1376. <https://doi.org/10.1016/j.compositesa.2005.08.016>.
- [27] K. L. Pickering, G. W. Beckermann, S. N. Alam, N. J. Foreman, *Compos. A* **2007**, 38, 461. <https://doi.org/10.1016/j.compositesa.2006.02.020>.
- [28] V. Stepanova, P. Slavicek, M. Stupavska, J. Jurmanova, *Appl. Surf. Sci.* **2015**, 355, 1037. <https://doi.org/10.1016/j.apsusc.2015.07.121>.
- [29] M. A. Cuiffo, J. Snyder, A. M. Elliott, N. Romero, S. Kannan, G. P. Halada, *Appl. Sci.* **2017**, 7(6), 579. <https://doi.org/10.3390/app7060579>.
- [30] J. M. Chacón, M. A. Caminero, E. Garcia-Plaza, P. J. Nuñez, *Mater. Design.* **2017**, 124(15), 143. <https://doi.org/10.1016/j.matdes.2017.03.065>.
- [31] D. Li, Y. Jiang, S. Lv, X. Liu, J. Gu, Q. Chen, Y. Zhang, *PLoS One* **2018**, 13(3), e0193520. <https://doi.org/10.1371/journal.pone.0193520>.
- [32] X. Cao, A. Mohamed, S. H. Gordon, J. L. Willet, D. J. Sessa, *Termochim. Acta* **2003**, 406, 115. [https://doi.org/10.1016/S0040-6031\(03\)00252-1](https://doi.org/10.1016/S0040-6031(03)00252-1).
- [33] T. Tabi, I. E. Sajo, F. Szabo, A. S. Luyt, J. G. Kovacs, *EXPRESS Polym. Lett.* **2010**, 4(10), 659. <https://doi.org/10.3144/expresspolymlett.2010.80>.
- [34] M. A. Abselwahab, A. Flynn, B. S. Chiou, S. Imam, W. Orts, E. Chiellini, *Polym. Degrad. Stab.* **2012**, 97, 1822. <https://doi.org/10.1016/j.polymdegradstab.2012.05.036>.
- [35] X. Yongfu, Z. Yi, *Text. Res. J.* **2019**, 90(13–14), 1628. <https://doi.org/10.1177/0040517519891449>.
- [36] C. R. Ribeiro de Castro Lima, L. D. Brocardo Machado, M. V. Robles Velasco, J. R. Matos, *J. Therm. Anal. Calorim.* **2018**, 132, 1429. <https://doi.org/10.1007/s10973-018-7095-0>.
- [37] J. Cao, F. Leroy, *Biopolymers* **2005**, 77, 38. <https://doi.org/10.1002/bip.20186>.
- [38] U. Ozmen, B. O. Baba, *J. Therm. Anal. Calorim.* **2017**, 129, 347. <https://doi.org/10.1007/s10973-017-6188-5>.
- [39] H. Y. Cheung, K. T. Lau, X. M. Tao, D. Hui, *Composites, Part B* **2008**, 39-6, 1026. <https://doi.org/10.1016/j.compositesb.2007.11.009>.
- [40] S. Cheng, K. T. Lau, T. Liu, Y. Zhao, P. M. Lam, Y. Yin, *Composites, Part B* **2009**, 40, 650. <https://doi.org/10.1016/j.compositesb.2009.04.011>.
- [41] H. S. Kim, B. H. Park, J. H. Choi, J.-S. Yoon, *J. App. Polym. Sci.* **2008**, 109, 3087. <https://doi.org/10.1002/app.28229>.

- [42] R. Masirek, Z. Kulinski, D. Chionna, E. Piorkowska, M. Pracella, *J. Appl. Polym. Sci.* **2007**, *105*, 255. <https://doi.org/10.1002/app.26090>.
- [43] B.-H. Lee, H.-S. Kim, S. Lee, H.-J. Kim, J. R. C. Dorgan, *Sci. Technol.* **2009**, *69*, 2573.
- [44] I. M. De Rosa, A. Iannoni, J. M. Kenny, D. Puglia, C. Santulli, F. Sarasini, A. Terenzi, *Polym. Compos.* **2011**, *32*, 1362. <https://doi.org/10.1002/pc.21159>.
- [45] L. E. Krause Sammartino, M. I. Aranguren, M. M. Reboredo, *J. Appl. Polym. Sci.*, **2010**, *115-4*, 2236. <https://doi.org/10.1002/app.31325>.
- [46] P. Srivastava, C. Kumar Garg, S. Sinha, *Mater. Today.* **2018**, *5-11*, 22922. <https://doi.org/10.1016/j.matpr.2018.11.019>.
- [47] M. Khan, M. Ali, *Constr. Build. Mater.* **2018**, *00166-30*, 581. <https://doi.org/10.1016/j.compositesb.2017.02.015>.
- [48] C. G. Flores-Hernandez, A. Colin-Cruz, C. Velasco-Santos, V. M. Castaño, J. L. Rivera-Armenta, A. Almendarez-Camarillo, P. E. Garcia-Casillas, A. L. Martinez-Hernandez, *Polymer* **2014**, *6*, 686. <https://doi.org/10.3390/polym6030686>.
- [49] A. Gregorova, M. Hrabalova, R. Wimmer, B. Saake, C. Altaner, *J. Appl. Polym. Sci.* **2009**, *114*, 2616. <https://doi.org/10.1002/app.30819>.
- [50] A. L. Martinez-Hernandez, C. Velasco-Santos, M. de Icaza, V. M. Castaño, *Composites, Part B* **2007**, *38*, 405. <https://doi.org/10.1016/j.compositesb.2006.06.013>.
- [51] F. P. Incropera, D. P. Dewitt, T. L. Bergman, A. S. Lavine, *Fundamentals of Heat and Mass Transfer*, John Wiley & sons, Inc., USA **2007**.
- [52] X. Huang, G. Liu, X. Wang, *Adv. Mater.* **2012**, *24*, 1482. <https://doi.org/10.1002/adma.201104668>.
- [53] M. S. Barkhad, B. Abu-Jdayil, M. Z. Iqbal, A. H. I. Mourad, *Constr. Build. Mater.* **2020**, *261*, 120533. <https://doi.org/10.1016/j.conbuildmat.2020.120533>.
- [54] R. Guo, Z. Ren, H. Bi, M. Xu, L. Cai, *Polymer* **2019**, *11(549)*, 1. <https://doi.org/10.3390/polym11030549>.
- [55] S. Kumar, R. Singh, T. P. Singh, B. A. J. Thermoplas, *Mater.* **2020**, *1*. <https://doi.org/10.1177/0892705720907651>.
- [56] F. C. Pai, H. H. Chu, S. M. J. Lai, *Elastom. Plast.* **2019**, *52(1)*, 53. <https://doi.org/10.1177/0095244318825286>.
- [57] N. Mao, S. J. Russell, *Text. Res. J.* **2007**, *77(122)*, 914. <https://doi.org/10.1177/0040517507083524>.
- [58] J. Gao, W. Yu, N. Pan, *Text. Res. J.* **2007**, *77-8*, 617. <https://doi.org/10.1177/0040517507079408>.
- [59] U. Meyer, T. Meyer, J. Hanschel, H. P. Wiesmann, *Fundamentals of tissue engineering and regenerative medicine*, first ed., Springer-Verlag, Berlin **2009**.
- [60] P. Hill, H. Brantley, M. V. Dyke, *Biomaterials* **2010**, *31*, 585. <https://doi.org/10.1016/j.biomaterials.2009.09.076>.
- [61] K. K. Nayak, P. Gupta, *Int. J. Biol. Macromol.* **2015**, *81*, 1. <https://doi.org/10.1016/j.ijbiomac.2015.07.025>.
- [62] Y. Yu, R. Cui, X. Wang, H. Yang, H. Li, *Int. J. Biol. Macromol.* **2020**, *155*, 14. <https://doi.org/10.1016/j.ijbiomac.2020.03.180>.
- [63] G. Lin, H. Zhou, J. Lian, H. Chen, H. Xu, X. Zhou, *Colloids and Surface B: Biointerfaces* **2019**, *175*, 291. <https://doi.org/10.1016/j.colsurfb.2018.11.074>.
- [64] M. I. Bajestani, S. Kader, M. Monavarian, S. Mohammad, E. Jabbari, A. Jafari, *Int. J. Biol. Macromol.* **2020**, *142*, 790. <https://doi.org/10.1016/j.ijbiomac.2019.10.020>.
- [65] E. Fortunati, A. Aluigi, I. Armentano, F. Morena, C. Emiliani, S. Martino, C. Santulli, L. Torre, J. M. Kenny, D. Puglia, *Mat. Sci. Eng. C-Mater* **2015**, *47*, 394. <https://doi.org/10.1016/j.msec.2014.11.007>.
- [66] R. K. Perumal, S. Perumal, R. Thangam, A. Gopinath, S. K. Ramadass, B. Madhan, S. Sivasubramanian, *Int. J. Biol. Macromol.* **2018**, *106*, 1032. <https://doi.org/10.1016/j.ijbiomac.2017.08.111>.

#### SUPPORTING INFORMATION

Additional supporting information may be found online in the Supporting Information section at the end of this article.

**How to cite this article:** Flores-Hernandez CG, Velasco-Santos C, Rivera-Armenta JL, et al. Additive manufacturing of green composites: Poly (lactic acid) reinforced with keratin materials obtained from Angora rabbit hair. *J Appl Polym Sci.* 2020;e50321. <https://doi.org/10.1002/app.50321>